

IV-measurements of InP NW solar cells

Klara Novakova, Axel Sandberg

December 17, 2019

1 Introduction

In this study, the I-V characteristics both in the dark and under illumination of nanowire InP solar cells were obtained with a probe station. By analysing the resulting I-V curves, parameters such as the saturation current I_s , ideality factor η , maximum output power P_{max} and filling factor FF were attained. Moreover, Electron Beam Induced Current measurement (EBIC) was done on single InP nanowires in order to obtain their I-V characteristics as well as the current distribution in the nanowire.

2 Theory

The building blocks of the solar cells studied were InP nanowires each consisting of a p-i-n junction. A p-i-n junction consists of three regions as suggested by the acronyms; p-doped region, intrinsic region (undoped) and n-doped region. The p-doped region is created by introducing acceptor impurities (elements lacking an electron compare to the intrinsic material) while in the n-doped region donors (elements with an extra electron compare to the intrinsic material) are injected. As a result p-doped regions contains positively charged holes which are free to move in the lattice and n-doped region encompasses mobile electrons. When the three different regions are brought together, mobile charges start to migrate and recombine thus giving rise to a depletion region (region depleted of mobile carriers) shown in figure 1. As a result of the absence of mobile carriers in the depletion region, an electric field is formed by the ionised donors and acceptors. It is this electric field in the depletion region that plays the main role in the current generation of a solar cell.

When photons hit the solar cell and are subsequently absorbed, they generate electron-hole pairs by exciting the electrons from the valence band to the conduction band. If an electron-hole pair is created in the depletion zone, the electric field pulls the electrons and holes towards contacts on opposite sides of the cell as shown in figure 1. The electrons are accelerated towards the n-side and the holes to the p-side and thus a photocurrent is generated by the cell. The same process would have occurred even if the intrinsic region was omitted and we instead had a p-n junction. However, the electric field in the depletion would be of a lower magnitude. Lower electric field would mean that less electrons/holes would be accelerated towards the contacts thus yielding a lower photocurrent. Therefore most solar cells consist of p-i-n junctions rather than p-n.

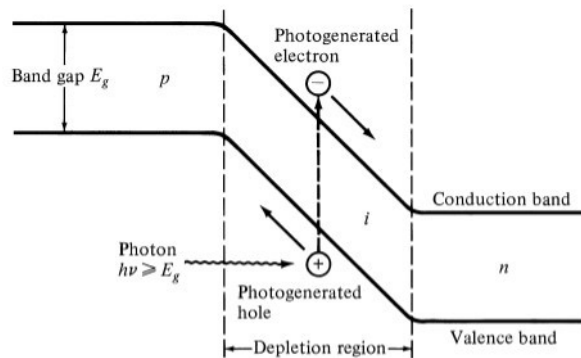


Figure 1: The mechanism of current generation in a p-i-n junction solar cell. Figure taken from [1].

When a solar cell is in the dark, its current-voltage (I-V) characteristic is identical to the one of a diode; a large current is observed when the forward bias is applied while in the case of the reverse bias, only very insignificant amount of current, called the saturation current I_s , flows through. The saturation current corresponds to the leakage of carriers across the p-i-n junction under reverse bias conditions. Thus the behaviour of a solar cell in the dark can be described by the ideal diode equation defined as followed,

$$I(V) = I_s (e^{V/\eta V_T} - 1), \quad (1)$$

where V is the voltage across the diode/solar cell, η is the ideality factor which describes how closely does the behaviour of a diode/solar cell match the theoretical model. The value of ideality factor ranges

from 1 to 2, where ideal diode has $\eta = 1$. Lastly, V_T is the thermal voltage in the diode/solar cell defined as $\frac{kT}{q}$, where k is the Boltzmann constant, T is temperature of the diode/solar cell in Kelvin and q is the elementary charge. By fitting Eq. 1 to the linear part of the dark I-V curve, one can obtain the ideality factor ν and the saturation current I_s .

Alternatively, the ideal diode equation can be simplified by making the last term equal to zero if we only consider a forward biased region of the I-V curve. Such approximation yields,

$$I(V) = I_s(e^{V/\eta V_T}), \quad (2)$$

where if take a natural logarithm of both sides we get

$$\ln(I(V)) = \frac{1}{\eta V_T}V + \ln(I_s), \quad (3)$$

which is an equation of a line. By plotting the the I-V curve with a logarithmic scale on the y-axis and fitting equation 3, one can obtain the ideality factor η from the gradient of the line and I_s from the y-intercept.

Conversely, when a solar cell is illuminated, the I-V curve is shifted in the direction of the negative current I by an amount I_L as shown in figure 2. When the voltage across the solar cell is zero, the current is at its maximum possible value, short circuit current I_{sc} . On the other hand a maximum voltage, known as the open circuit voltage V_{oc} , is measured when no current flows through the cell. The aim is to achieve the highest possible power output P_{max} , where

$$P_{max} = I_{mp}V_{mp}, \quad (4)$$

where I_{mp} and V_{mp} are the optimal operation values of the current and voltage. The I-V plot is a very useful tool for this task, as one can find the optimal operation values of the current and voltage, I_{mp} and V_{mp} , of the cell yielding the desired maximal power output as illustrated in figure 2 by the dashed rectangle.

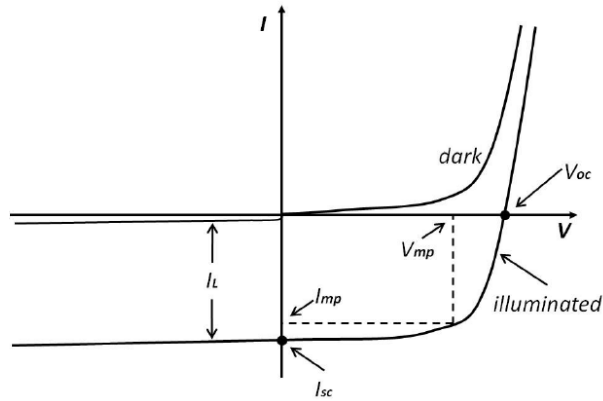


Figure 2: Figure taken from [2]

An important measure of solar cells quality is then the filling factor defined as,

$$FF = \frac{P_{max}}{P_T} = \frac{I_{mp}V_{mp}}{I_{sc}V_{oc}}, \quad (5)$$

where P_T is the theoretical maximum power generated by a solar cell and $P_T = I_{sc}V_{oc}$. The filling factor ranges from 0 up to 100%.

2.1 EBIC

Electron Beam Induced Current (EBIC) is a technique that enables the measurement of the electric properties of a semiconductor. For this project it was used to measure the I-V characteristics of single InP nanowires (NW) as well as the current distribution in the NW. EBIC works in a similar fashion as a regular solar cell as described above, with the exception that electron-hole pairs are generated

by an electron beam rather than by photon excitation. EBIC measurements are usually performed in a Scanning Electron Microscope (SEM). A probe is then connected to one end of the NW while it is scanned by an electron beam. The conductive properties in each region of the NW can thus be visualised as a contrast image by the SEM. This also gives an indication of any defects present in the sample.

3 Method

The I-V characteristics of 4 different solar cells from the sample in figure 3 both in the dark and under illumination were measured using a probe station. The cells were chosen such that a variety of size and overall cell quality was covered. Thus we chose two small cells, x4y3a and x4y3d, where x4y3d was slightly damaged. For the larger cells, x4y2 and x4y4 were chosen, where x4y4 was bonded to the back contact.

The EBIC measurements were conducted in a SEM. The solar cell made up of an InP substrate covered by InP NW was cut in half in advance by the supervisor and placed on a sample holder. The sample was inserted into the SEM and the cut side was investigated because the growth length of the NW was more easily controlled in the centre of the underlying substrate. A probe with a tip-diameter around 150 nm was connected to the top of a NW. The I-V characteristics in both dark and light conditions (active SEM probe). The current generated in the NW was also recorded while being hit by an electron gun. A contrast SEM image could thus be constructed were the current generated in the NW was plotted as a function of length.

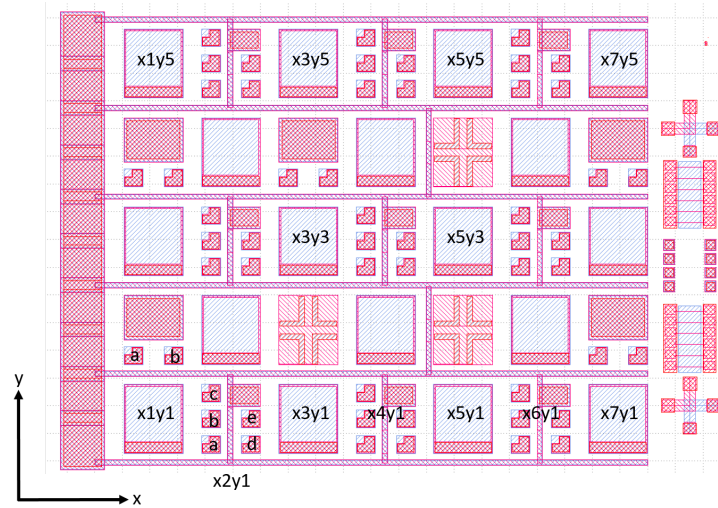


Figure 3: The map of the sample with a range of solar cells used in the I-V measurements.

4 Results and Discussion

4.1 I-V Characteristics obtained with the probe station

The I-V characteristics in the dark of the solar cells studied are shown in figure 4. One can observe that the current under reverse bias does not reach a plateau as expected. And therefore we could not conclude any exact values of the saturation current directly from the plot. However, the I_s values were obtained by fitting the deal diode equation to the data as shown in appendix in figure 11. The values summarised in table 1 show that the saturation current values are several orders of magnitude lower than the current values under reverse bias as observed in the plots in figure 4. This could be caused by severe leakage current due a poor sample manufacturing. All four solar cells measured had an ideality factor η greater than 1.7 and thus showed that they very poorly resemble a diode. The two larger cells, x4y2 and x4y4 had the worse ideality factor. This could be due to a higher chance of contamination of the larger cells as compare to the smaller cells.

Cell	η	I_s [A]
x4y3d	1.8250	$1.7692 \cdot 10^{-11}$
x4y3a	1.7918	$1.2387 \cdot 10^{-11}$
x4y2	2.2136	$1.2613 \cdot 10^{-9}$
x4y4	2.2271	$1.3665 \cdot 10^{-9}$

Table 1: The values of the saturation current I_s and ideality factor η obtained by fitting Eq. 1

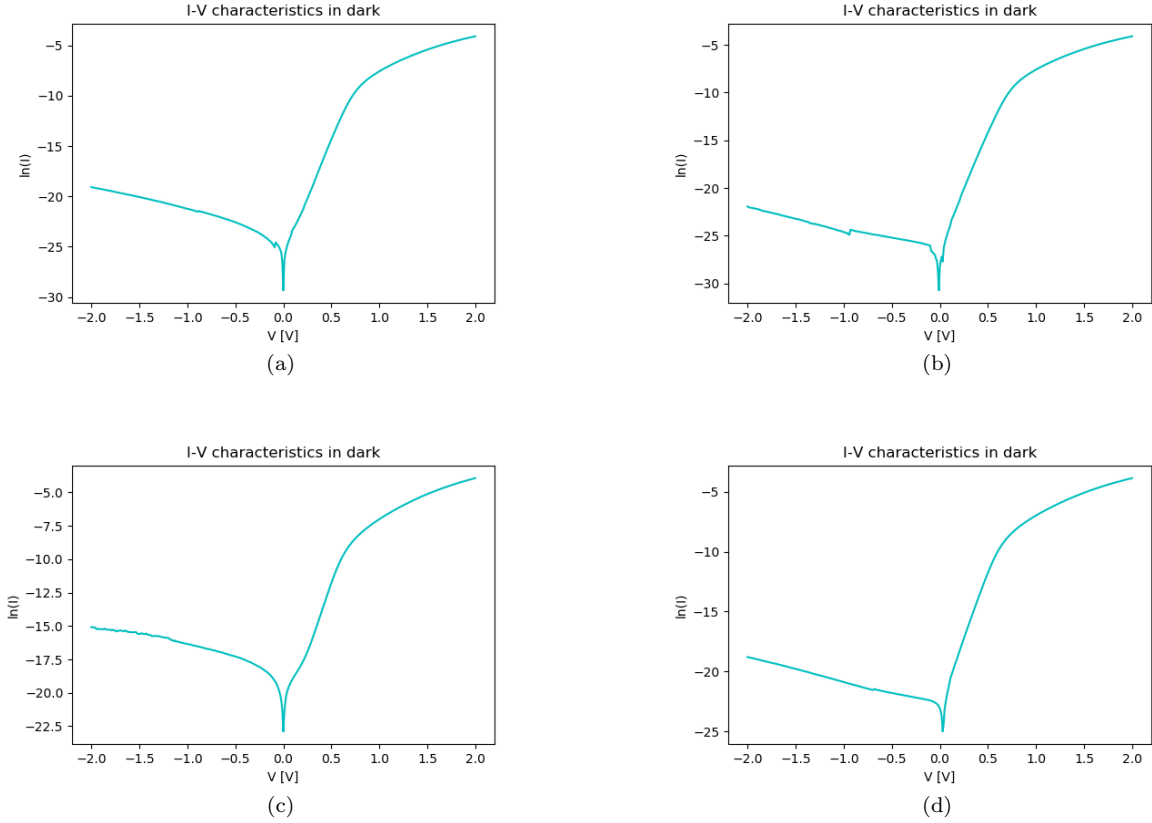


Figure 4: The I-V characteristics in dark of (a)x4y3a cell, (b)x4y3d cell, (c)x4y2 cell and (d) x4y4 cell.

The I-V characteristics of two of the solar cells under illumination are presented in figure 5. From there V_{OC} and I_{SC} could be extracted and P_{max} , P_T and FF could be calculated as described in the theory section. These values are all displayed in table 2. There are a couple of things affecting a solar cells quality such as resistances in the circuit and defects. By comparing the FF 's of each of the solar cells we can observe that the highest FF was obtained by the x4y3a cell, it was thus the most effective cell of this measurement. The other small cell, x4y3d, had a bit lower FF , which can probably be explained by that it had taken some damage. The difference between x4y2 and x4y4 can most likely be explained by the fact that x4y2's conducting plate was bonded by an aluminium wire. The highest power P_{max} was obtained by x4y4 and how it was calculated can be seen in figure 6. This value easily be compared to the one of x4y2 since they had the same surface area and indicated that x4y4 is able to output a higher current while having the same voltage applied over it, making it more effective.

Cell	V_{OC} [V]	I_{SC} [A]	P_{max} [W]	P_T [W]	FF [%]
x4y3a	0.40	7.2718e-08	1.8798e-08	2.9087e-08	64.63
x4y3d	0.40	7.91e-08	1.9691e-08	3.1634e-08	62.25
x4y2	0.43	2.7476e-06	6.9024e-07	1.1815e-06	58.42
x4y4	0.44	2.7797e-06	7.4599e-07	1.2230e-06	60.99

Table 2: Observed parameters of the solar cells, obtained under illumination. Presented are also the calculated P_{max} , P_T and FF

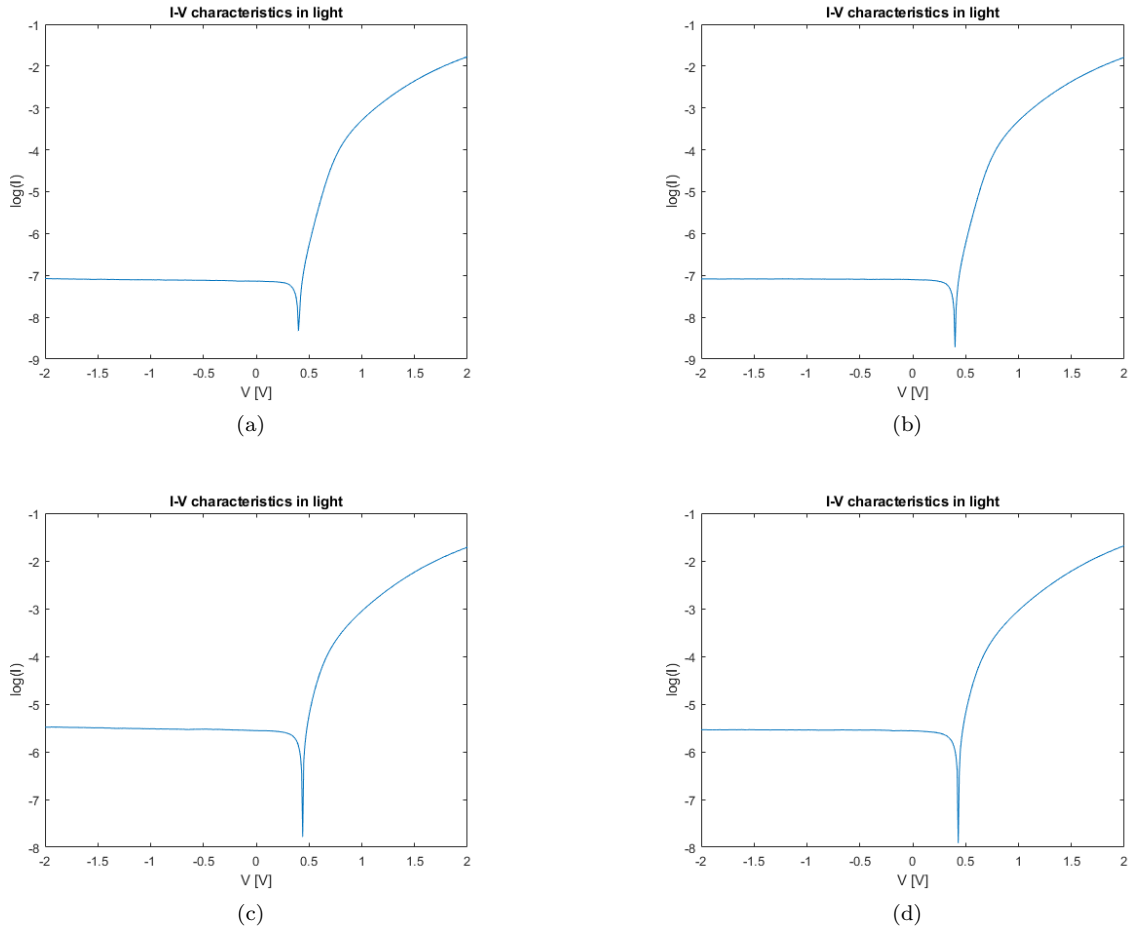


Figure 5: The I-V characteristics in light of (a)x4y3a cell, (b)x4y3d cell, (c)x4y2 cell and (d) x4y4 cell.

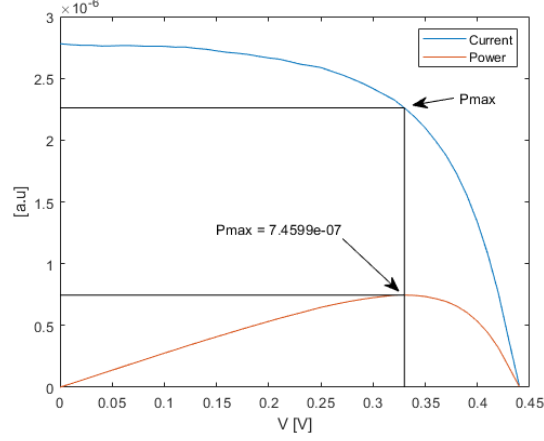


Figure 6: Showing the process of the Pmax calculation in the x4y4 cell. Pmax indicates the maximum area under the I-V plot and thus the "squareness" of the curve.

4.2 EBIC measurement

Figure 7 shows the results of the I-V measurement on the individual NW while being hit by the electron gun. The results of the calculations of the I-V characteristics are presented in table 3. Figure 8 shows the I-V characteristics of the nanowires in dark, from there the ideality factor and saturation current could be extracted, presented in table 4. Very high ideality factors were calculated for both of the NW making them poorly resemble a diode. This might be explained by the oxide deposited on top of the NW, which resulted in a poor contact with the probe.

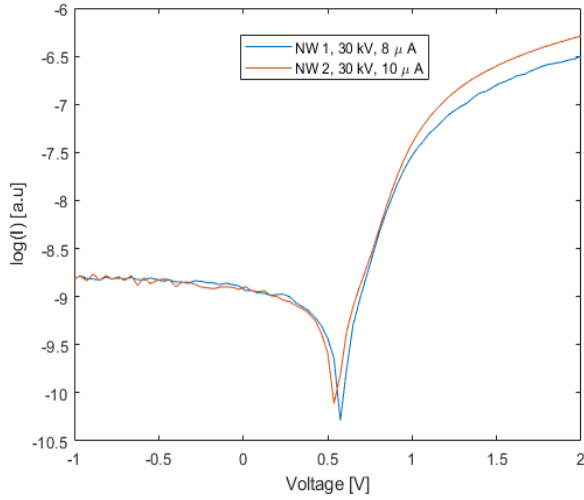


Figure 7: I-V characteristics for the single nanowires while being hit with the electron gun.

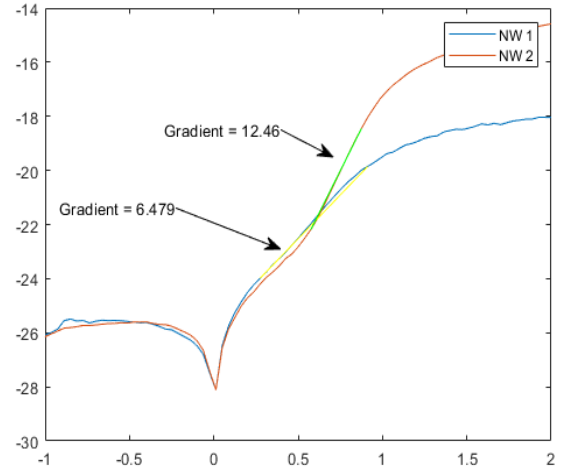


Figure 8: I-V characteristics for the single nanowires in dark conditions.

NW	V_{OC} [V]	I_{SC} [A]	P_{max} [W]	P_T [W]	FF [%]
1	0.5749	1.1545e-09	2.7572e-10	6.6374e-10	41.54
2	0.5374	1.2709e-09	2.6276e-10	6.8300e-10	38.47

Table 3: Observed parameters of the single nanowires, obtained under electron gun exposure. Presented are also the calculated P_{max} , P_T and FF .

NW	η	I_s [A]
1	5.9696	$6.4949 \cdot 10^{-12}$
2	3.1041	$1.7925 \cdot 10^{-13}$

Table 4: The values of the saturation current I_s and ideality factor η obtained by fitting Eq. 3.

Figure 9 and 10 shows the plotted contrast image taken in the SEM while the NW was hit by the electron gun. The current generated was thus plotted as a function of length of the NW. The current generation is very concentrated towards the top of the wire, where the probe was attached. This was probably due to our inexperience with handling the measurement probe. The measurements made took too long, exposing the NW to the light of the SEM for quite long periods of time, which led to charge build-up in the oxide layer.

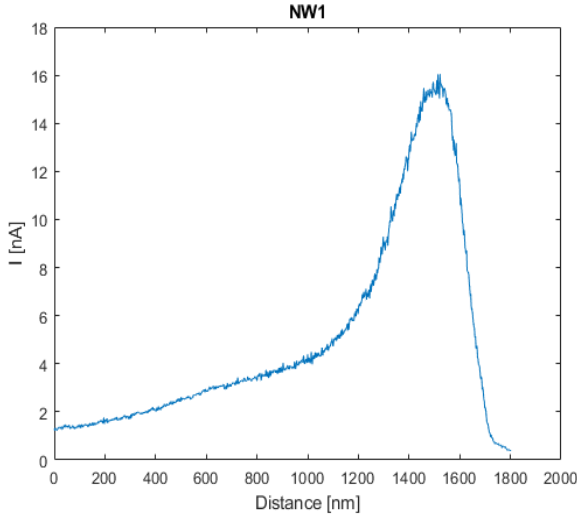


Figure 9: The current generated in NW 1 plotted over the total length of the wire.

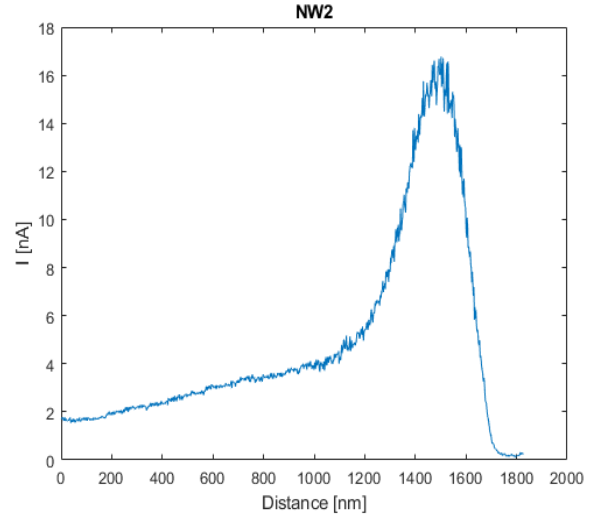


Figure 10: The current generated in NW 2 plotted over the total length of the wire.

Reference

[1] K.Rajagopal, *Textbook of Engineering Physics*, PHI Learning Pvt. Ltd., 2012.

[2] P. S. Priambodo, N. R. Poespawati and D. Hartanto, *Solar Cells - Silicon Wafer-Based Technologies*, InTech, 2011,

Available from: <http://www.intechopen.com/books/solar-cells-silicon-wafer-based-technologies/solar-cell>.

Appendix

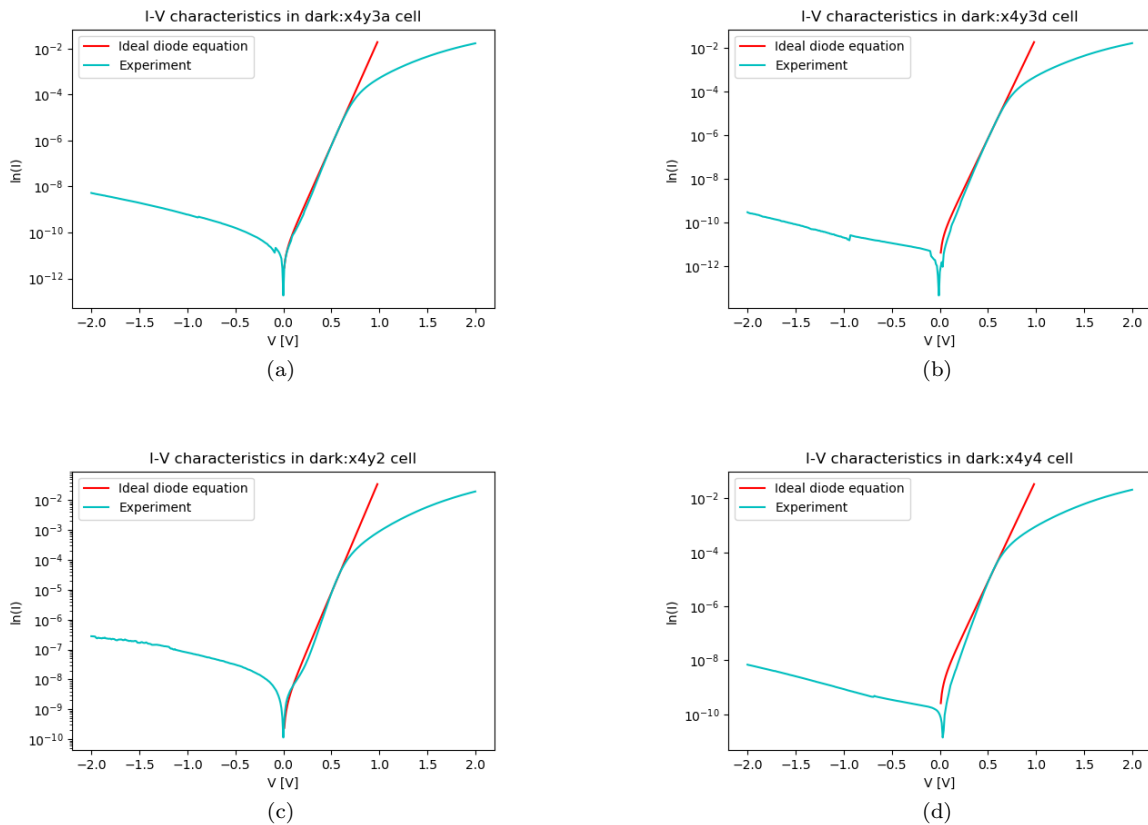


Figure 11: The I-V curves under no illumination fitted with the ideal diode equation under forward bias approximation from Eq. 1, where (a)x4y3a cell, (b)x4y3d cell, (c)x4y2 cell and (d) x4y4 cell.